

MAQ-CaF: A Modular Air Quality Calibration and Forecasting method for cross-sensitive pollutants

Yousuf Hashmy, *Student Member, IEEE*, Zill Ullah Khan, *Student Member, IEEE*, Rehan Hafiz, *Member, IEEE*
Usman Younis, *Senior Member, IEEE* and Tauseef Tauqeer, *Member, IEEE*

Abstract—The climatic challenges are rising across the globe in general and in worst hit under-developed countries in particular. The need for accurate measurements and forecasting of pollutants with low-cost deployment is more pertinent today than ever before. Low-cost air quality monitoring sensors are prone to erroneous measurements, frequent downtimes, and uncertain operational conditions. Such a situation demands a prudent approach to ensure an effective and flexible calibration scheme. We propose MAQ-CaF, a modular air quality calibration, and forecasting methodology, that side-steps the challenges of unreliability through its modular machine learning-based design which leverages the potential of IoT framework. It stores the calibrated data both locally and remotely with an added feature of future predictions. Our specially designed validation process helps to establish the proposed solution’s applicability and flexibility without compromising accuracy. CO, SO₂, NO₂, O₃, PM_{1.0}, PM_{2.5} and PM₁₀ were calibrated and monitored with reasonable accuracy. Such an attempt is a step toward addressing climate change’s global challenge through appropriate monitoring and air quality tracking across a wider geographical region via affordable monitoring.

Index Terms—Low cost sensors and devices, sensor calibration, cloud services and air quality.

I. INTRODUCTION

GLOBALLY, around 90% of the population breathe air that is non-compliant with WHO Air Quality Guidelines, resulting in a loss of around 3 million human lives annually [1]. Moreover, degradation in air quality poses an imminent threat to work efficiency and economy as well, as indicated in [2], [3]. Less economically developed countries (LEDCs) are adopting low-cost sensing techniques to enhance spatio-temporal data density, without exceeding financial limitations [4], [5]. One of the challenges faced by employing IoT-based low-cost sensor networks is the accuracy of measurements. Lately, the quality of information (QoI) metrics of such networks has transformed into an area of keen interest [6]. Low-cost sensors are prone to erroneous readings, generally [7]–[9]. To address the issues pertaining to the calibration of air quality metrics based upon IoT, researchers and scientists have been focusing on laboratory calibration [7] or co-location calibration [10]–[12]. The former involves standard gas mixtures and superior-quality analytical instruments. Additionally, the non-linearities in the real measurements are not easily achieved in a controlled laboratory environment. The latter uses the references from some government-run systems to calibrate the low-cost sensors. The datasets are often made public such as EPA AirNow. In [13], the co-located instruments have shown promise in calibrating NO₂ and O₃. Furthermore, [14] discusses the edge-computing infrastructure for the monitoring

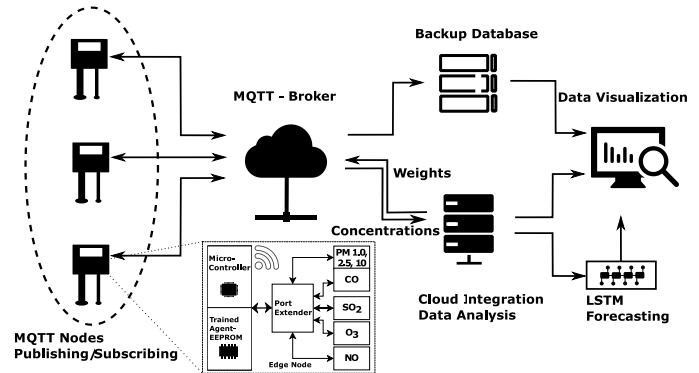


Fig. 1. The platform for monitoring and calibration of pollutant concentration on a large scale. Each sensor edge node consists of a micro-controller, a EEPROM, a port extender and air quality sensing elements.

of air quality indicators. The details of cost comparisons of various platforms are provided in [14], alluding to cost-effectiveness, and ease of implementation. The fusion of the data acquired from multi-sensor IoT platform for metal-oxide and electrochemical sensors for only two kinds of pollutants is described in [15], [16]. [15] further indicates the need for the cross-sensitivity of the air quality indicators. Additionally, the work in [17], discusses static as well as mobile air monitoring systems subject to their respective deployment strategies. The portal system requires larger logistics and increased costs. The inflexibility of the pollution monitoring and calibration schemes are also some of the major concerns [17].

The measurements of the low precision sensor nodes (LPNs) have non-linearities and uncertainties due to a poor measuring accuracy [18]. The simpler calibration methods such as polynomial curve fitting methods [19], utilized in past could not produce the desired results because of the complexity of the problem. Support vector machines have also been employed in this field [20]. K-Nearest Neighbors and random forest approaches are also being adopted in the past [15]. In [21], the methods of uni-variable and multi-variable neural network regression techniques were implemented. However, those methods did not incorporate the cross-sensitivity between different air quality parameters. In [22], the authors have implemented some complex non-linear models, however, they are limited to only two pollutants and the methods are less practical and more analytical.

The past work is unable to address the issues of frequent downtimes and intermittent data-stream at any given time. To overcome the gaps in past work, we aim to present a modular air quality calibration method which readily adjusts according to the availability of measurement sources. Additionally, the design considers the inter-dependency of the pollutants and the climatic parameters. Due to the reliability limitations of low-cost sensors, the data required for incorporating cross-

sensitivity may not be available at all times. This demands an adjustable design for the platform that consists of a multi-topic MQTT (Message Queuing Telemetry Transport) broker [23]. Model-based application of MQTT are explained in [24]. We leverage the real-time monitoring through this protocol similar to the approach pursued in [23]. The to and fro data transfer helps to get the best-learned weights to the edge module inside the sensor nodes and enables the data to be received at the local database and data processing servers. A calibrator is programmed on each sensor node that comprises of four stages depending upon the data from various sensors. All the stages are powered by trained machine learning agents. The first stage considers each air quality measure separately; the second considers the environmental parameters such as temperature, pressure, and relative humidity. The third stage is designed to incorporate the cross-sensitivity of different air quality factors for the gas-based sensors. Lastly, the fourth layer combines both the gas sensor data and particulate matter data to maximize the information gain because there is evidence of cross-correlation between them [25]. A specialized scheme is adopted to select the models through a micro-controller. We extend our method to provide near-accurate predictions of the future as well. For that reason, we apply a mutual information score-based feature selection and long short term memory-based learning agents.

The rest of this paper is organized as follows. Section II gives details of MAQ-CaF, i.e., our calibration and prediction scheme. Section III entails the modeling and problem definition. Section IV and V delve into the calibration methodology and model selection, respectively. Section VI discusses the forecasting methodology, Section VII provides the validation of the proposed methods, and section VIII concludes the paper.

II. CALIBRATION AND MONITORING

We propose a decentralized calibration method where the sensor nodes are capable of displaying the pollutant concentrations locally as well as populating sensor values on the remote data integration server.

IoT technology is the backbone of such a strategy. Bi-directional communication mode is adopted, and its security is studied in detail in [26]. In this scheme, one topic of MQTT is reserved for each direction. The publishers are the sensing nodes while the subscribers are the backup and cloud-integration databases, for one of these directions. Two databases enhance the redundancy to avoid data loss in case of any contingency and cyber-attack. Machine learning models are used for learning the calibration models in the cloud. Moreover, integrated cloud also behaves as a publisher, and the subscribers are the sensor nodes. The weights of the learned models are updated using this channel. Once the weights matrix is updated, the calibrated pollutant concentrations are populated on the sensing nodes, immediately. The weights need an update rarely as compared to pollutant concentration data being transmitted to the databases.

Fig. 1 provides a detailed illustration of the calibration and forecasting scheme. A multi-topic broker helps to provide services for air quality parameters as well as the calibration

models and their weights. For each node, the PM and gas pollutants' concentrations are recorded and the micro-controller loads the trained calibration agent from cloud integration layer onto the electronically erasable programmable read-only memory (EEPROM). The calibrated readings are published to the MQTT-broker.

III. MODELLING FOR CALIBRATION

The article aims to propose an effective technique for the calibration of LPNs by exploiting the high fidelity data obtained from high-cost (by order of magnitude) and high precision sensor nodes HPNs. With such an objective in perspective, we propose a modular air quality calibrator and forecaster scheme, MAQ-CaF, as illustrated in Fig. 2. We define the input form a low-cost sensor array comprising of the sensor output from either the gas-based sensors $C_i \in \mathbb{R}^t$ for $i \in [1, 2, 3, \dots, n]$ number of sensors, or the particulate matter based sensors $P_j \in \mathbb{R}^t$ for $j \in [1, 2, 3, \dots, m]$ number of sensors, where $t \in [1, 2, 3, \dots, T]$ indicates all the time points. Similarly, we specify the outputs of the learning mechanism $C_{i,cal} \in \mathbb{R}^t$ and $P_{j,cal} \in \mathbb{R}^t$. Subsequently, for the convenience we combine the sensor inputs and output as $S_{in} \in [C_i^{(t)}, P_j^{(t)}]$ and $S_{out} \in [C_{i,cal}^{(t)}, P_{j,cal}^{(t)}]$. To keep the approach modular, the calibration is carried out in four stages $X \in [X1, X2, X3, X4]$, with each stage comprising multiple calibration agents. The agents are learned during a training phase using the historical target data comprising of C_i^* and P_j^* readings provided by the HPNs. Moreover, weather parameters such as temperature tm_i and $tm_j \in \mathbb{R}^t$, pressure pr_i and $pr_j \in \mathbb{R}^t$ and relative humidity hm_i and $hm_j \in \mathbb{R}^t$ in the surroundings of i -th or j -th sensor are also leveraged to boost up the calibration performance. The calibrated measurements S_{out} are subject to the forecasting architecture to generate $C_{i,pred}^{(t)}$ and $P_{j,pred}^{(t)}$ for a pre-specified number of days.

A. Problem Definition

Problem: design an effective calibration mechanism without compromising on the flexibility of the technique. A generalized approach is presented.

Given:

- an LPN L for measuring $n + m$ different pollutants, giving C_i and P_j real-time measurements with frequent downtimes
- temperature tm_i and tm_j , atmospheric pressure pr_i and pr_j and relative humidity hm_i and hm_j measurements with random downtimes, and
- an HPN H with historical measurements C_i^* and P_j^* of $n + m$ number of different pollutants.

To Find:

- calibrated LPN measurements $C_{i,cal}^{(t)}$ and $P_{j,cal}^{(t)}$ for gaseous and particular matter sensors,
- modular design of the calibrator to achieve flexibility, and
- forecast estimates $C_{i,pred}^{(t)}$ and $P_{j,pred}^{(t)}$ for a specified number of days ahead.

IV. CALIBRATION TECHNIQUES

MAQ-Caf consists of multiple calibration stages (X1, X2, X3, and X4) each comprising one or more

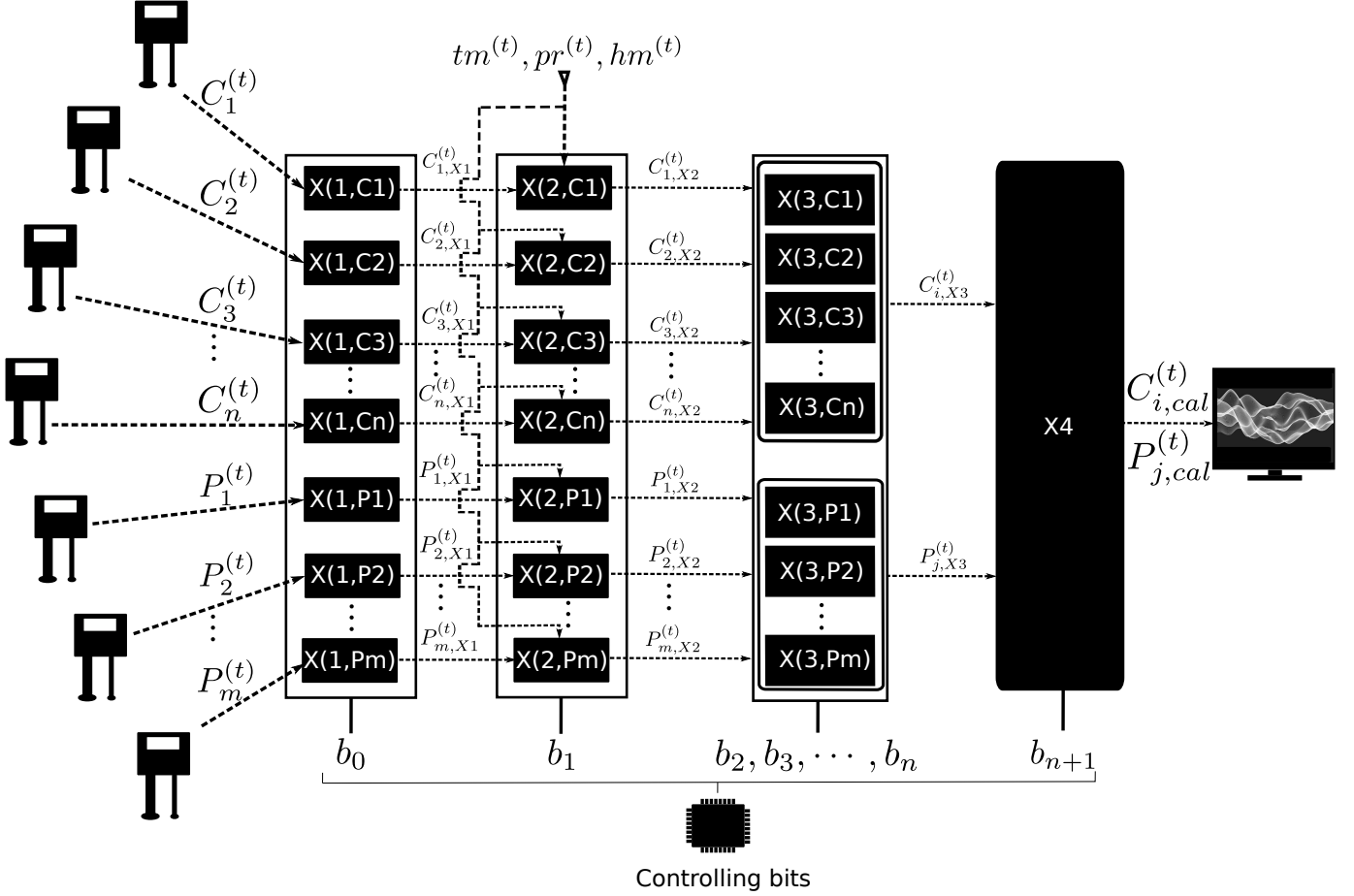


Fig. 2. Architecture of the proposed MAQ-CaF scheme. Here, the trained agents are labelled as $X(\text{stage number, input air quality metric})$. The modular technique involves multiple calibrating agents and a controller. Stage X1 requires only the S_{in} to give the estimating of each air quality measure. Stage X2 takes in the estimation from the previous stage and environmental factors $tm^{(t)}$, $pr^{(t)}$ and $hm^{(t)}$. Stage X3 and stage X4 uses multiple pollutants for leveraging cross-sensitivity among them. Any stage can be enabled at any time using its enable controlling bit, as per requirement and availability of data.

calibration agents. Once the trained weights of a learned calibration agent are available, the calibration can be applied in real-time depending upon the controllers' output $B \in [0, 1]^{n+m+5}$. For training purposes, an LPN node is co-located with an HPN for an extended time period (~ 6 Months), and the acquired data is logged on the server. This is done for the atmospheric data and the smog constituents: CO, SO₂, O₃, NO and PM_x concentrations. The time points are averaged over a period of 1 hr for the training purpose. In the following, we provide a brief of each of the calibration techniques evaluated for the proposed MAQ-CaF scheme.

A. Support Vector Regression

For each sensor i or j , there exists a sensor output from both LPN and HPN to be used for training. Each one of them represents a feature in a higher dimensional space generated by the SVR (Support Vector Regression) model, as purported in [27]. A mapping rule \mathcal{F}_C and \mathcal{F}_P for the measurement of gases and particulate matter is then established between LPN and HPN readings.

$$\mathcal{F}_C : C_i \rightarrow C_{i,X}; \mathcal{F}_P : P_j \rightarrow P_{j,X}. \quad (1)$$

In an SVR model the weights vector ω_i is indicative of the slope of dividing hyperplane and the feature space is selected to keep the separation at maximum for all time points $t \in [0, 1, 2, \dots, T]$. The optimization function is,

$$\min \left(\frac{1}{2} \|\omega_i\|_2 + \gamma \sum_{t=1}^T \zeta_i^{(t)} \right), \quad (2)$$

where $\zeta_i^{(t)}$ controls the hard or soft margin in case of the non-separable environment in the newly created feature space, and $\gamma \in \mathbb{R}^2$ in the range of $[0, 1]$. The gaussian kernel was selected for the experimentation for CO, SO₂, O₃, NO₂, and PM_x.

B. Random Forest

Random Forest is an ensemble-based algorithm for regression and has been a prudent selection in the past [27] for calibration of PM_{2.5} values. Considering Q number of decision trees, the output is obtained through,

$$C_{i,X}^{(t)} = \frac{1}{Q} \sum_{q=1}^Q \text{tree}_X^{(t)} \quad (3)$$

A similar procedure repeats for $P_{j,X}^{(t)}$. We employ standard grid search for evaluating the hyper-parameters through cross-validation.

C. K-Nearest Neighbors

In K-Nearest Neighbor's feature space, the closest K points to S_{in} are used for training purposes, for every X . Their Euclidean distances are used to ascertain the K distinct neighboring samples in \mathbb{K} . Finally, their mean is evaluated to get the result for both $C_{i,X}^{(t)}$ and $P_{j,X}^{(t)}$. Hence, $C_{i,X}^{(t)} = \frac{1}{k} \sum_{C_i^{(t)} \in \mathbb{K}} C_i^{(t)}$.

D. Multivariate Linear Regression

Multivariate Linear Regression is a simple yet promising linear regression technique for multiple feature variables. The weight arrays α_i and α_j for each kind of air quality metric are learnt by minimizing the euclidean distance from the regressed hyper-plane so, $C_{i,X}^{(t)} = \sum_i \alpha_i \cdot C_i^{(t)}$. The data from gas-based and particular matter-based sensors are subjected to the same procedure.

E. Deep Neural Networks

Apart from the classical Machine Learning based methods, as discussed above, we also explored deep neural networks. Owing to the richness of information provided by the correlating gases and the particulate matter data, a deep neural network may better recognize the complicated patterns and improve the calibration accuracy.

$$C_{i,X}^{(t)} = \sum_i \phi_{xp}(\Omega_i \cdot C_i^{(t)}); P_{j,X}^{(t)} = \sum_j \phi_{xp}(\Omega_j \cdot P_j^{(t)}) \quad (4)$$

where ϕ_{xp} represents the activation functions, and xp is the number of perceptrons. Moreover, Ω_i and Ω_j indicate the weights learned during the training process. Deep neural networks present an apt solution to such regression problems where there exist highly complex and non-linear patterns in different air quality measures. The activation function types, loss function types, and the number of hidden layers and their perceptron counts are determined through a k-fold cross-validation method.

V. MODEL SELECTION

MAQ-CaF has a modular design comprising multiple stages and their associated calibration agents, as shown in Fig. 2. These calibrating agents are selected from the various learned models described in the last section. Note that these learning agents have different performances at different stages. Some agents may show superior performance under fewer input features, while others may be better with denser and larger input feature space. With that in consideration, we propose a model selection approach guided by an evaluation metric to achieve the sub-optimal calibration while preserving the flexibility.

Having the calibration results for each of the learning method invokes a need for a metric of evaluation. The evaluation of the calibration of environmental sensors has long been performed via the root mean squared error (RMSE) method. If the real measurements from an HPN are $C_{i,X_{real}}^{(t)}$ and $P_{j,X_{real}}^{(t)}$, the error functions are defined as,

$$\text{RMSE}_{C_i}^X = \sqrt{\frac{1}{T} \sum_{t=1}^T (C_{i,X}^{(t)} - C_{i,X_{real}}^{(t)})^2}, \quad (5)$$

$$\text{RMSE}_{P_j}^X = \sqrt{\frac{1}{T} \sum_{t=1}^T (P_{j,X}^{(t)} - P_{j,X_{real}}^{(t)})^2}. \quad (6)$$

In stages X1 and X2, all agents are trained using each of the proposed calibration method, individually. We adopt a specially designed optimization function for selecting the model with the least RMSE_C and RMSE_P , accordingly. For

all the trained models m , $M_i \in \mathbb{R}^m$ has the RMSE values of those models for C_i inputs. Similarly, $N_j \in \mathbb{R}^n$ holds the RMSE values of the n trained models for P_j inputs of stage 1. The following optimization function delivers the argument of the model with the best performance in stage X1.

$$\arg \min_{M_i} b_0 \cdot \sum (\text{RMSE}_{M_i}) \quad (7)$$

$$\arg \min_{N_j} b_0 \cdot \sum_{N_j} (\text{RMSE}_{N_j}) \quad (8)$$

where b_0 is the controlling bit which can either be 0 (stage is disabled) or 1 (stage is enabled).

For stage X2, the process of model selection is repeated in the same way, with additional features being appended namely $tm^{(t)}$, $pr^{(t)}$, and $hm^{(t)}$ for incorporating the environmental factors. That is because the literature claims the interdependence of air quality metrics and environmental factors. Hence, when the bit b_1 is set to 1 the outputs are populated as $C_{i,X2}^{(t)}$ and $P_{j,X2}^{(t)}$.

Stage 3 is unique in its design and implementation because here, all the data available for all the n gasses is taken in to consideration. Since we are aiming for a modular design, we consider the likelihood of not having the incoming data for all the gases because of any logistical, cost and network accessibility constraints. In such a case, the past estimation $C_{i,X2}^{(t)}$ or $P_{j,X2}^{(t)}$ serves as the input and the controller enables one of the two blocks. Bits b_2 and b_3 control the blocks at stage 3 as depicted in Table I.

TABLE I
CONTROLLING STAGE 3 BLOCKS.

b_2	b_3	$C_{i,X3}$	$P_{j,X3}$
0	0	Disable	Disable
0	1	Disable	Enable
1	0	Enable	Disable
1	1	Enable	Enable

In addition to b_2, b_3 , stage X3 further provides a finer level of control using the controlling bits $b_4, b_5, \dots, b_{n+m+4}$, for providing increased sensor flexibility through modular design. Stage X3 comprises two blocks. One of the blocks has a maximum of n number of inputs, while the other block has a maximum of m number of inputs. Since there exists a likelihood of unavailability of any of the input parameters, we design the calibration mechanism to account for all the possible cases. For the block with inputs $C_{i,X2}^{(t)}$, the total number of possible combinations of inputs is u , similarly for the block with inputs $P_{j,X2}^{(t)}$, it is v . Then, the total number of models is w ,

$$u = \sum_{i=1}^n \binom{n}{i} - n; v = \sum_{j=1}^m \binom{m}{j} - m, \quad (9)$$

$$w = u + v = \sum_{i=1}^n \binom{n}{i} + \sum_{j=1}^m \binom{m}{j} - (n + m), \quad (10)$$

where $(.)$ indicates the function for evaluating combinations. Hence, X3 can have any possible combination of their respective inputs with the exception of single input features because those cases have already been taken care of in X1 and X2

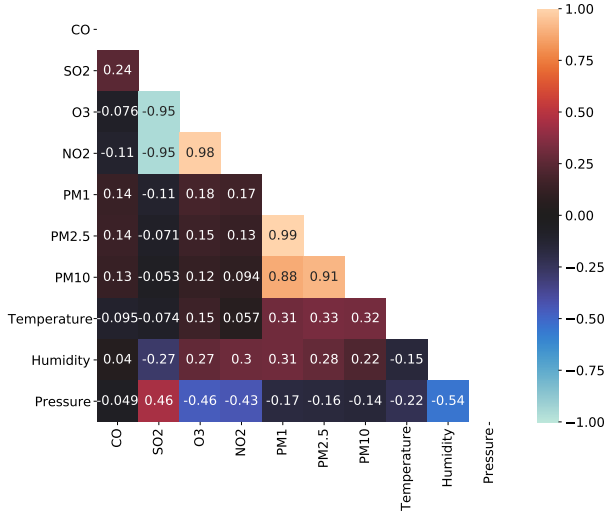


Fig. 3. Pearson's Correlation Coefficients corresponding to different air quality parameters.

stages. Similar to the expressions (7) and (8), we use the RMSE values to select the best of all the pre-trained calibration models for making appropriate predictions.

$$\arg \min_{M_i} b_2 \cdot \sum_{M_i} (\text{RMSE}_{M_i}) \quad (11)$$

$$\arg \min_{N_j} b_3 \cdot \sum_{N_j} (\text{RMSE}_{N_j}) \quad (12)$$

The output of this stage will be the nearly calibrated $C_{i,X3}^{(t)}$ and $P_{j,X3}^{(t)}$. For most of the air quality parameters, this stage can serve as the final state. However, considering the recent findings of cross-sensitivity between the gas and PM sensors, there can be another stage, taking advantage of the cross-correlations between PM_x and gaseous pollutants of the LPN. The enable bit b_{n+m+5} helps to bypass (0) or activate (1) the single block X4 of stage X4. The process for model selection for this stage is similar to that of stages X1 and X2, where the calibration models were selected through the RMSE minimization. Since only a single block exists at stage X4, for each $C_{i,X4}^{(t)}$ a total of only m agents are trained and only one of them is selected for making future inferences, in case of each input to deliver the result of either $C_{i,cal}^{(t)}$ or $P_{j,cal}^{(t)}$.

This article proposes a methodology that is highly modular and flexible in nature. It can effectively be reduced to any level of learning without a significant rise in the RMSE (drop in performance) as demonstrated later in Section VII. The method is successful in delivering reliable calibration results even under the constraints such as unavailability of other air quality parameters or climatic factors. These characteristics render the proposed solution to be flexible. It also enables us to exploit the simple as well as complex machine learning capabilities which were mostly ignored in such a problem in the past, such as the introduction of deep learning that has proven to be most effective under rich data scenarios. The effectiveness of the methodology is trialled through rigorous testing and validation as demonstrated later in Section VII.

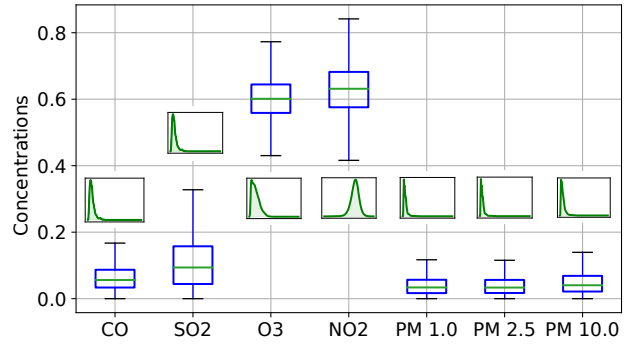


Fig. 4. Distribution and box-whisker plots of the normalized air quality metrics' concentrations for comparative analysis.

VI. FORECASTING THROUGH LSTM

The calibrated measurements $C_{i,cal}^{(t)}$ and $P_{j,cal}^{(t)}$ are stored in the cloud integration database where the data is further processed to predict the future trends of the air quality parameters. Such an analysis is instrumental in taking preemptive measures, accordingly. LSTM-based networks are widely employed for time series predictions. We propose to establish a generic architecture for determining effective feature set. The correlation matrix provides an insight into the linear cross-correlations only, whereas, $C_{i,cal}^{(t)}$ and $P_{j,cal}^{(t)}$ of different air quality parameters have non-linear correspondence as well. To capture the non-linear dependencies, we propose a solution based upon the mutual information score $I_{(s,s')}$ between any two features in the feature pool, as in [28]. Since I has the capability to capture the non-linear dependencies also, it is a naturally preferred choice. $H(\cdot)$ gives the entropy of a random variable,

$$I_{(s,s')} = H(S_s) + H(S_{s'}|s' \neq s) - H(S_s, S_{s'}|s' \neq s), \quad (13)$$

where $s \in [1, 2, \dots, n+m]$ is the subscript of the air quality parameter to be forecast and $s' \in [1, 2, \dots, n+m+3]$ is the representative of all the other features in the feature pool to include all the gaseous and particulate matter air quality parameters along with the three environmental factors of temperature, pressure and relative humidity. Our goal is to select the features having highest mutual information scores with the parameter to be forecast. Therefore, for each air quality parameter s ,

$$\arg \max_{|L|=l} \sum_{s' \in L} I_{(s,s')}, \quad (14)$$

we get the l features with highest mutual information scores with the air quality parameter to be calibrated. The selected number of features l depends upon the computational capabilities and resource availability. It is advised to adopt a cross-validation mechanism to ascertain that number.

We get the features and feed them as input to the multivariate-LSTM for making predictions. In [29], a comprehensive methodology is proposed focused on modelling LSTM for forecasting of air quality measures. We obtain the output h_t of the LSTM through its cell state, that combines the cell state C_t and output gate o_t , as depicted in Fig. 5. We denote weights matrix by W_C and biases by b_C .

$$C_t = f_t \cdot C_{t-1} + i_t \cdot \tanh(W_C[h_{t-1}, X_t] + b_C), \quad (15)$$

$$h_t = o_t \cdot \tanh(C_t) \quad (16)$$

Finally, fully connected layers are added to the network to train the agent to get $S_{pred}^{(t)} \in [C_{i,pred}^{(t)}, P_j, pred^{(t)}]$.

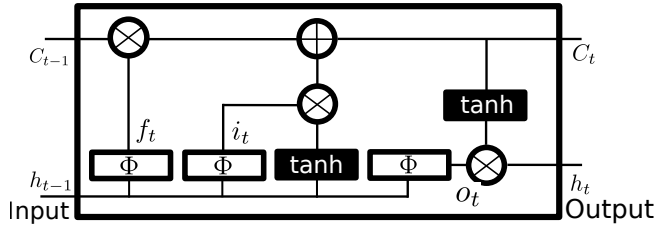


Fig. 5. A single unit of LSTM carrying tanh and sigmoid activation functions.

VII. NUMERICAL VALIDATION

With a well-defined model of the proposed calibrator and forecaster, we proceed to validate the efficacy and reliability of the methods as discussed in the previous sections for collocation-based calibration and forecasting.

A. Developing Sensing System

We design a low-cost sensing system by leveraging digital electro-chemical SPEC Sensors (DGS-CO-968 – 034, DGS-NO2-968–043, DGS-SO2-968–038, and DGS-O3-968–042). Moreover, we mount the PMS 7003 on each sensor node assembly. Such sensors determine the particulate matter concentration by optical variations. Their low cost and better spatio-temporal resolution makes them a suitable fit for this study [30]. To reduce the cost of production, we employ an ESP32 micro-controller. We utilize a port extender for Universal Asynchronous Receiver/Transmitter (UART) communication to overcome the port limitation challenge. Fig. 6 shows our developed LPN, a low-cost sensing node with components as referenced in Fig. 1. Furthermore, we employ two co-located Libellium Smart Environment Pro kits [31] as HPNs. The factors for selecting that product is its ease of IoT integration, longer life, and performance stability guarantees. The sensor nodes are located at $31^{\circ}28'32.82''N$ and $74^{\circ}20'33.13''$ in Lahore, Pakistan. The LPN and HPN are incorporated in the same installation. We recorded and used the measurements of 6 months from February, 2019 to July, 2019 for the analysis and validation. Table II provides the detailed description of the data under consideration. LPN is the low precision node, and HPN-1 and HPN-2 are the two high precision nodes.

TABLE II
DATA DESCRIPTION.

Source	Approx. Resolution (measurements/minute)	Data Dropout Approx. %	Bad Data Approx. %
LPN	0.5	8	12
HPN-1	1	2	< 1
HPN-2	1	< 1	1

The calibration mechanisms as adopted in the past lack the information enrichment capability through the interdependence of the chemical components that constitute the smog. To overcome such issues, we collect the data of past 6 months for different air quality metrics including

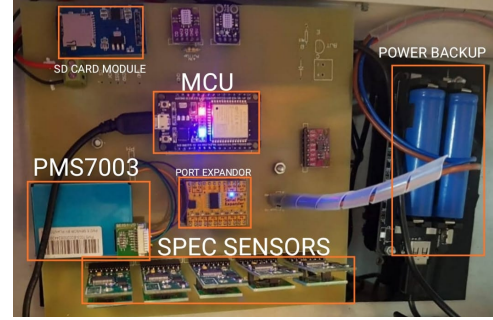


Fig. 6. A low-cost sensor node containing SPEC and PMS 7003 sensors along with the communication assembly (ESP32) capable to interacting with MQTT-broker. It has a micro-control unit (MCU), local storage capability in the form of SD-card module, and a power backup.

CO, SO₂, NO₂, O₃, PM_{1.0}, PM_{2.5} and PM₁₀. We conduct a correlation analysis of the air quality metrics to validate the claim using HPN data. Fig. 3 illustrates the heat map of Pearson's correlation among the considered environmental as well as air quality parameters. The heat map shows that there exists a strong correlation between some of the features, e.g., a high value of 0.95 exists between NO₂ and SO₂. By considering the additional information of cross-sensitivity of air quality parameters, the performance of the calibration is enhanced substantially. Furthermore, the variances and means of different air quality measures are slightly dissimilar but their distributions are related to each other, as shown in Fig. 4. Particulate matter sensors have closely related data distributions among themselves. CO and SO₂ have a high degree of similarity too. These observations provide a rich evidence for utilizing their cross-sensitivities while designing the calibrator. The discrepancies in the low-cost LPNs result in missing values. The missing values are removed. In order to correct the measurements, a mean over an extended time is taken in [19]. Moreover, [32] presents a methodology using 1 measurement per hour. We adopt a similar approach by averaging the data over past 1 hour.

B. Validation - Stage X1

The past research on the calibration of the air quality parameter sensing mostly considers only single parameter, which is under study. We show that behavior in the form of X1 models for CO, SO₂, NO₂, O₃, PM_{1.0}, PM_{2.5} and PM₁₀. In [19], PM_{2.5} is calibrated by developing only a 2 dimensional space of calibrated and un-calibrated readings for a particular interval of time. Similarly, [15], [33] propose methods for self calibration only. We develop the solution based upon that as a benchmark for comparison. Moreover, it is the only possible way to accomplish a reasonable estimation when only a single quantity is measured without access to environmental factors like temperature, pressure, and relative humidity. It is shown in Fig. 7. Except for PM_{1.0} and CO, a fully connected deep neural network shows a superior calibration result. Since the dimensionality of the feature space is very limited, KNN and SVR also perform well. X1 is thus useful for feature deficient cases.

C. Validation - Stage X2

Drawing inspiration from [11] and reproducing its results simply with temperature as an additional parameter would

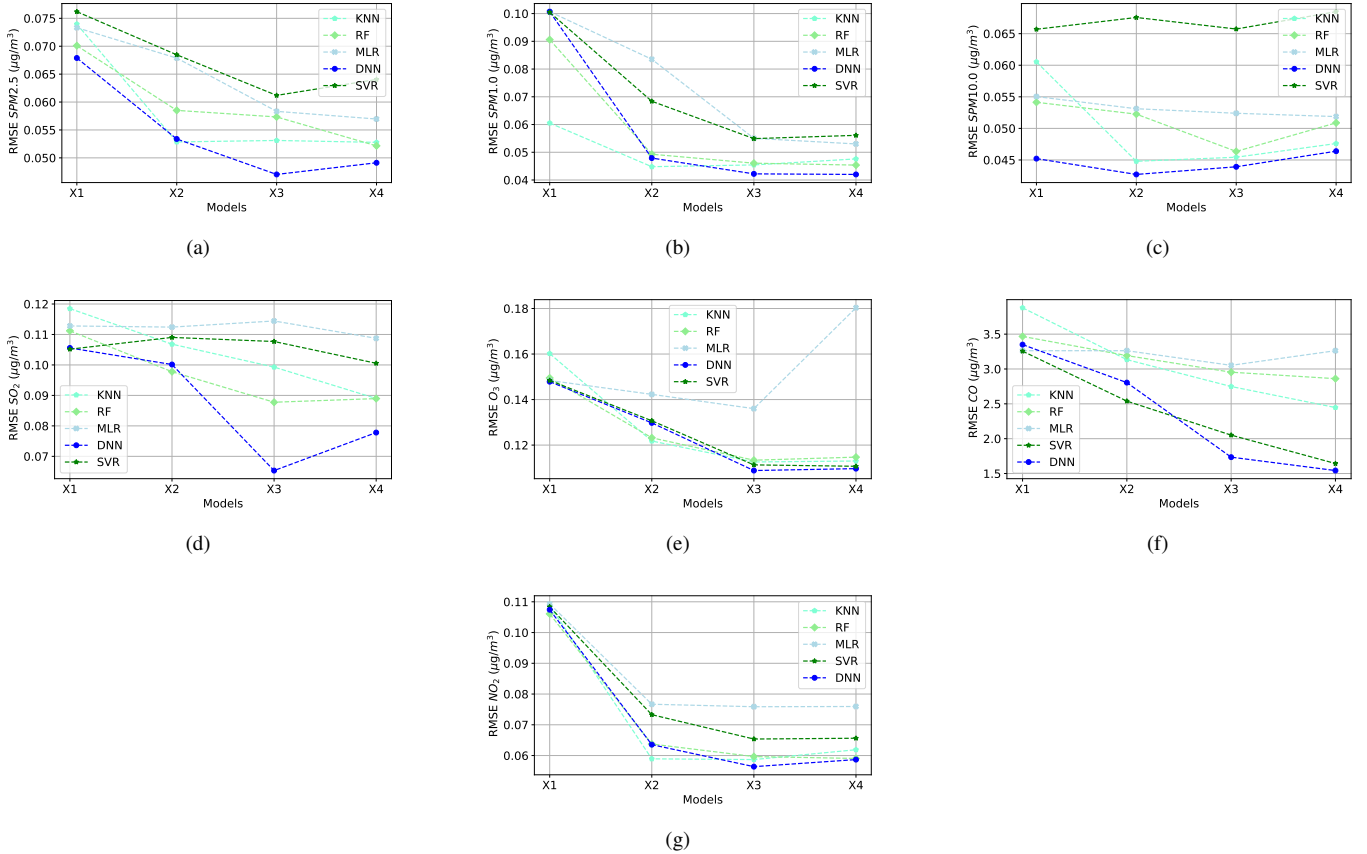


Fig. 7. RMSE values of all the models at levels X1, X2, X3, X4 corresponding to the respecting air quality parameter.

not have been a smart choice. Fig. 3 illustrates that not only does temperature have a stark correlation with air quality parameters, but the pressure and relative humidity also do. Therefore, for the calibration at stage X2, a strategy was employed to incorporate those environmental factors. It is enabled only when those factors are available to be utilized for making appropriate inferences. Interestingly, PM_{10} has the least RMSE at the X2 stage when DNN was selected as the model. It can be explained through the behavior of the data under consideration where the PM_{10} has the least cross-sensitivity. We implement the calibrator so that the output with the least RMSE is always returned as the final result. The cross-sensitivity has no role to play up to this stage. It serves the purpose of enhanced flexibility well, as it is likely for some cases where there exist only the environmental factors and not the other air quality measures. In such scenarios, the preceding stages shall be bypassed.

D. Validation - Stage X3

There is largely a void in the previous work on pivoting the cross-sensitivity of several air quality measures while calibrating the LPNs. In [11], the researchers allude to this fact but only as a potential future work. We tend to develop a holistic approach with maximum information exploitation. The interdependence of the parameters is indicated in Fig. 3 as Pearson's correlation coefficients. Moreover, the datasheets of SPEC-sensors also provide analytical evidence of the cross-sensitivity of air quality measures. Subfigures 7a, 7b, 7c, 7d, 7e, 7f, and 7g depict the improvement in the perfor-

mance of calibrators and validate the performance of proposed methodology. The only anomaly is PM_{10} , where we observed a relatively low RMSE due to the low interdependence of PM_{10} on the others. Also, due to the existence of numerous air quality indicators, the model selection method searches for a larger space in this case. The number of combinations of input features can be $11 + 4 = 15$ because there are 4 inputs corresponding to SPEC sensors and 3 to PM sensors. Intuitively, fully connected tuned deep neural networks are the best learners in this space. The dimensionality of the data is high; consequently, more complex features can be learned [34]. This approach, in conjunction with the control mechanism, epitomizes the modularity of the calibrator. Irrespective of which of the two or more air quality parameters are present, the proposed solution selects the best possible combination of inputs and the model. Since the model's selection is completed in the training phase, the size of the trained model is suitable to be deployed on-chip or in the server. In the worst case, the size DNN model is 2.5 kB for NO_2 , and for weights it is 823 kB. So the total size is 825.5 kB. For 7 sensors $825.5 \times 11 = 9080.5$ kB. Such a model can easily be deployed on most edge devices including ESP32 (with 16 MB EEPROM).

E. Validation - Stage X4

The past work in air quality measures has shown keen interest in the interdependence of some of the gases and particulate matter. The research work presented in [35] and [36] points out the relationship between $\text{PM}_{2.5}$ and CO. Stage

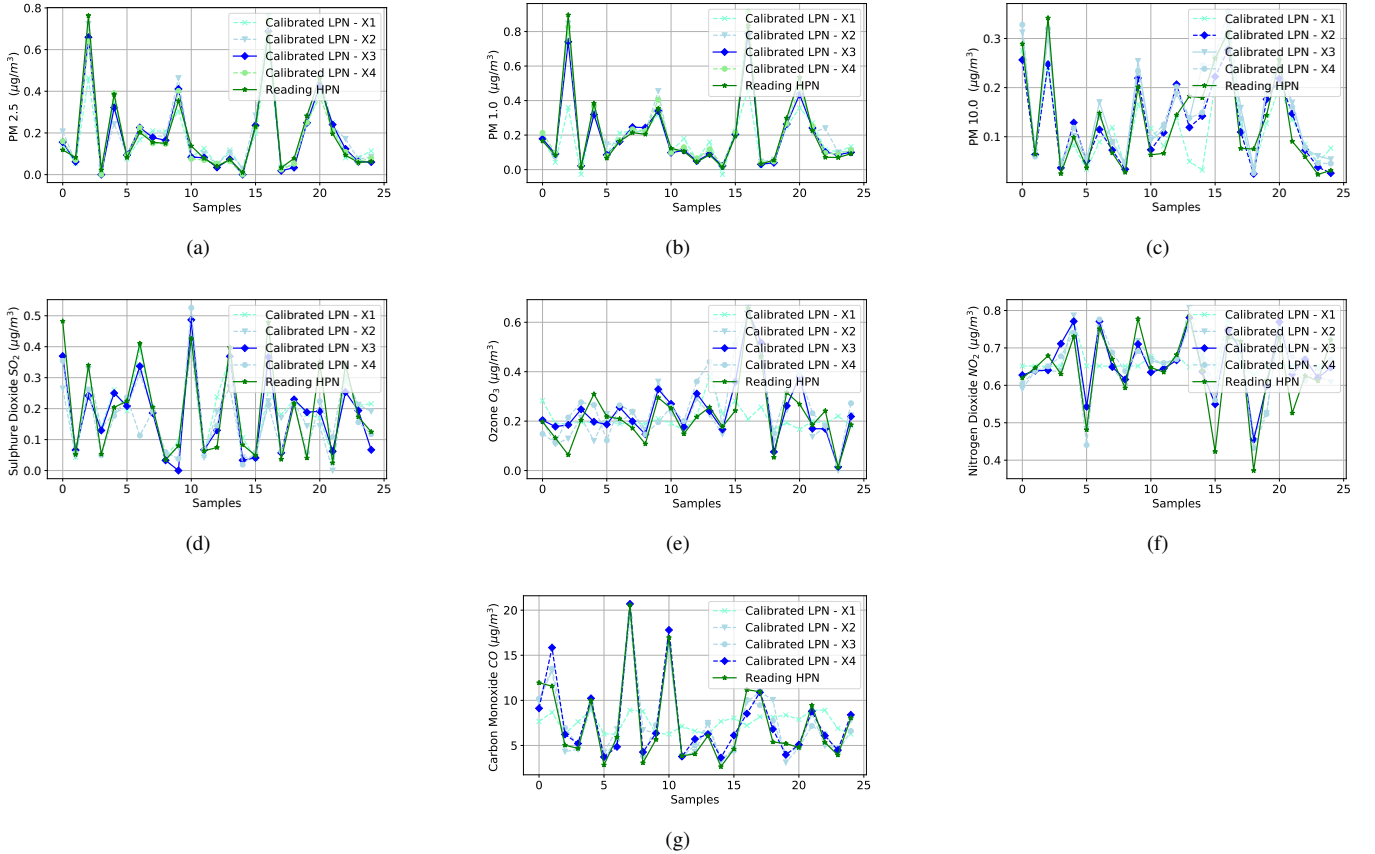


Fig. 8. Time samples of calibrated signals at stages X1, X2, X3, X4 corresponding to the respecting air quality parameter.

X4 is driven by that motivation. $PM_{1.0}$ and CO have shown a significant drop in RMSE. Whereas, for O_3 , the RMSE experiences a marginal drop, as shown subfigures 7b, 7e and 7f. The bit b_{n+m+5} bypasses the block when it is set to 0; otherwise, it performs its operation depending upon the respective RMSE. Furthermore, the best performing models for the appropriate input combination results in encouraging results in the time domain. Fig. 8 presents the time samples representing the hours of a day. The proposed methodology maintains a high fidelity for all the air quality parameters. Specifically, the calibration results of the PM sensors are most effective as illustrated in subfigures 8a, 8b and 8c. The patterns are well learned due to lesser uncertainty. Moreover, the calibrated results of SPEC sensors are presented in subfigures 8d, 8e, 8f and 8g. Since the model has the capability to gather the output for each stage (X1, X2, X3, and X4), the stage with the best output is selected as the final calibrator, and the corresponding model parameters are transmitted to the edge devices via MQTT-broker.

F. Validation - Forecasting

Finally, the calibrated readings are fed to a separate agent inside the cloud integration server to select the relevant features based upon mutual information score. Those relevant features help to train a multivariate-LSTM model. Table III provides the results in the form of RMSEs of the real and predicted values. Furthermore, a comparison with the approaches adopted in the past is also provided. It is evident from table III that the SO_2 and NO_2 have not been reliably forecasted in the past as they have not yet been calibrated and predicted

through modern machine learning tools. In conjunction with the LSTM core, our proposed feature selection methodology can enhance the accuracy many folds. The trend of predicted values for particulate matter are also dependable to a good extent as the r^2 values are above 80 in all the cases.

TABLE III
AIR QUALITY METRIC FORECAST.

Air Quality Metric	Proposed Architecture		Past Work
Chemical Formula	RMSE	r^2	RMSE
SO_2	0.02	0.96	17.42 [37]
CO	0.004	0.75	0.342 [38]
NO_2	0.72	0.61	25.40 [37]
O_3	0.050	0.92	2.36 [39]
$PM_{1.0}$	0.028	0.99	-
$PM_{2.5}$	0.061	0.96	0.092 [40]
$PM_{10.0}$	2.66	0.81	26.8 [41]

VIII. CONCLUSION

We implement a flexible calibration and forecasting scheme for affordable smog monitoring, that effectively employs IoT architecture. The scheme provides measurement and calibration setup for smog-causing pollutants, namely, CO, SO_2 , NO_2 , O_3 , $PM_{1.0}$, $PM_{2.5}$ and PM_{10} . We demonstrate that utilizing the cross-sensitivity of different air quality parameters during the later stages of our multi-stage calibration procedure allows flexible and affordable monitoring of smog constituents. To improve up the measurement accuracy of LPNs, we propose a flexible MAQ-CaF to enhance flexibility. The bidirectional and multi-topic capabilities of MQTT-broker are proposed for co-location calibration. MAQ-CaF can exploit tuned-machine

learning techniques enabled through a systematically designed model selection methodology based upon the availability of data from specific low-cost sensors. The systematic validation results depict the reduced RMSE at the stages X1, X2, X3, and X4 for the pollutants under consideration. Moreover, the encouraging results of the forecast of air quality parameters for the future are determined by mutual information score-based feature selection method and multivariate-LSTM. The technique can be effectively utilized in the developing world to improve their air quality tracking capability by leveraging IoT and flexible MAQ-CaF for detecting smog constituents in a wide geographic region.

REFERENCES

- [1] W. H. Organization *et al.*, "Ambient air pollution: A global assessment of exposure and burden of disease," *World Health Organization*, 2016.
- [2] U. Jaimini *et al.*, "Investigation of an indoor air quality sensor for asthma management in children," *IEEE Sensors Letters*, vol. 1, no. 2, pp. 1–4, 2017.
- [3] S. H. Ali and J. A. P. de Oliveira, "Pollution and economic development: an empirical research review," *Environmental Research Letters*, vol. 13, no. 12, p. 123003, 2018.
- [4] S. Munir, M. Mayfield, D. Coca, S. A. Jubba, and O. Osammor, "Analysing the performance of low-cost air quality sensors, their drivers, relative benefits and calibration in cities—A case study in Sheffield," *Environmental monitoring and assessment*, vol. 191, no. 2, p. 94, 2019.
- [5] A. Kumar and B. Gurjar, "Low-cost sensors for air quality monitoring in developing countries—a critical view," *Asian Journal of Water, Environment and Pollution*, vol. 16, no. 2, pp. 65–70, 2019.
- [6] P. Ferrer-Cid *et al.*, "A comparative study of calibration methods for low-cost ozone sensors in iot platforms," *IEEE Internet of Things Journal*, vol. 6, no. 6, pp. 9563–9571, 2019.
- [7] N. Castell *et al.*, "Can commercial low-cost sensor platforms contribute to air quality monitoring and exposure estimates?" *Environment international*, vol. 99, pp. 293–302, 2017.
- [8] C.-T. Chiang, "Design of a high-sensitivity ambient particulate matter 2.5 particle detector for personal exposure monitoring devices," *IEEE Sensors Journal*, vol. 18, no. 1, pp. 165–169, 2017.
- [9] K. R. Mallires, D. Wang, V. V. Tipparaju, and N. Tao, "Developing a low-cost wearable personal exposure monitor for studying respiratory diseases using metal-oxide sensors," *IEEE Sensors Journal*, vol. 19, no. 18, pp. 8252–8261, 2019.
- [10] F. Delaine, B. Lebental, and H. Rivano, "In-situ calibration algorithms for environmental sensor networks: A review," *IEEE Sensors Journal*, vol. 19, no. 15, pp. 5968–5978, 2019.
- [11] D. H. Hagan, G. Isaacman-VanWertz, J. P. Franklin, L. M. Wallace, B. D. Kocar, C. L. Heald, and J. H. Kroll, "Calibration and assessment of electro-chemical air quality sensors by co-location with regulatory-grade instruments," *Atmospheric Measurement Techniques*, 2018.
- [12] R. Sahu *et al.*, "Robust statistical calibration and characterization of portable low-cost air quality monitoring sensors to quantify real-time O₃ and NO₂ concentrations in diverse environments," *Atmospheric Measurement Techniques Discussions*, pp. 1–27, 2020.
- [13] M. Mueller, J. Meyer, and C. Hueglin, "Design of an ozone and nitrogen dioxide sensor unit and its long-term operation within a sensor network in the city of Zurich," *Atmospheric Measurement Techniques*, vol. 10, no. 10, p. 3783, 2017.
- [14] X. Lai, T. Yang, Z. Wang, and P. Chen, "IoT implementation of kalman filter to improve accuracy of air quality monitoring and prediction," *Applied Sciences*, vol. 9, no. 9, p. 1831, 2019.
- [15] P. Ferrer-Cid and others., "Multisensor data fusion calibration in IoT air pollution platforms," *IEEE Internet of Things Journal*, vol. 7, no. 4, pp. 3124–3132, 2020.
- [16] Q. P. Ha, S. Metia, and M. D. Phung, "Sensing data fusion for enhanced indoor air quality monitoring," *IEEE Sensors Journal*, vol. 20, no. 8, pp. 4430–4441, 2020.
- [17] Z. Idrees and L. Zheng, "Low cost air pollution monitoring systems: A review of protocols and enabling technologies," *Journal of Industrial Information Integration*, vol. 17, p. 100123, 2020.
- [18] L. Spinelle, M. Gerboles, M. G. Villani, M. Aleixandre, and F. Bonavita, "Field calibration of a cluster of low-cost available sensors for air quality monitoring. part a: Ozone and nitrogen dioxide," *Sensors and Actuators B: Chemical*, vol. 215, pp. 249–257, 2015.
- [19] M. Badura, Batog, and others., "Evaluation of low-cost sensors for ambient PM 2.5 monitoring," *Journal of Sensors*, 2018.
- [20] R. Laref, E. Losson, A. Sava, and M. Siadat, "Support vector machine regression for calibration transfer between electronic noses dedicated to air pollution monitoring," *Sensors*, vol. 18, no. 11, p. 3716, 2018.
- [21] M. Badura, P. Batog, A. Drzeniecka-Osiadacz, and P. Modzel, "Regression methods in the calibration of low-cost sensors for ambient particulate matter measurements," *SN Applied Sciences*, vol. 1, no. 6, p. 622, 2019.
- [22] M. A. Zaidan, N. H. Motlagh, P. L. Fung, D. Lu, H. Timonen, J. Kuula, J. V. Niemi, S. Tarkoma, T. Petäjä, M. Kulmala *et al.*, "Intelligent calibration and virtual sensing for integrated low-cost air quality sensors," *IEEE Sensors Journal*, vol. 20, no. 22, pp. 13 638–13 652, 2020.
- [23] R. Atmoko, R. Riantini, and M. Hasin, "IoT real time data acquisition using MQTT protocol," in *J. Phys. Conf. Ser.*, vol. 853, no. 1, 2017.
- [24] K. Tanabe, Y. Tanabe, and M. Hagiya, "Model-based testing for mqtt applications," in *Joint Conference on Knowledge-Based Software Engineering*. Springer, 2020, pp. 47–59.
- [25] H. Fu, Y. Zhang, C. Liao, L. Mao, Z. Wang, and N. Hong, "Investigating PM 2.5 responses to other air pollutants and meteorological factors across multiple temporal scales," *Scientific Reports*, vol. 10, no. 1, pp. 1–10, 2020.
- [26] S. Andy, B. Rahardjo, and B. Hanindhito, "Attack scenarios and security analysis of MQTT communication protocol in iot system," in *IEEE International Conference on Electrical Engineering, Computer Science and Informatics*, 2017, pp. 1–6.
- [27] Y. Wang, Y. Du, J. Wang, and T. Li, "Calibration of a low-cost pm2. 5 monitor using a random forest model," *Environment international*, vol. 133, p. 105161, 2019.
- [28] M. Maciejewska and A. Szczurek, "Indoor air quality monitoring network design based on uncertainty and mutual information," in *SENSORNETS*, 2014.
- [29] X. Xu and M. Yoneda, "Multitask air-quality prediction based on lstm-autoencoder model," *IEEE Transactions on Cybernetics*, vol. PP, pp. 1–10, 10 2019.
- [30] K. Wang, F.-e. Chen, W. Au, Z. Zhao, and Z.-l. Xia, "Evaluating the feasibility of a personal particle exposure monitor in outdoor and indoor microenvironments in shanghai, china," *International journal of environmental health research*, vol. 29, no. 2, pp. 209–220, 2019.
- [31] L. Inc., "White paper: Libelium unites benefits of smart cities iot solutions for air quality monitoring," Libellium Inc., Zaragoza, Spain, Tech. Rep., 2018. [Online]. Available: <https://www.libelium.com/libeliumworld/libelium-unites-benefits-of-smart-cities-iot-solutions-for-air-quality-monitoring/>
- [32] B. G. Loh and G. H. Choi, "Calibration of portable particulate matter-monitoring device using web query and machine learning," *Safety and Health at Work*, vol. 10, no. 4, pp. 452 – 460, 2019.
- [33] J. M. Barcelo-Ordinas and others., "Self-calibration methods for uncontrolled environments in sensor networks: A reference survey," *Ad Hoc Networks*, vol. 88, pp. 142–159, 2019.
- [34] Y. LeCun, Y. Bengio, and G. Hinton, "Deep learning," *nature*, vol. 521, no. 7553, pp. 436–444, 2015.
- [35] S. Bartington, I. Bakolis, D. Devakumar, O. Kurmi, J. Gulliver, G. Chaube, D. Manandhar, N. Saville, A. Costello, D. Osrin *et al.*, "Patterns of domestic exposure to carbon monoxide and particulate matter in households using biomass fuel in Janakpur, Nepal," *Environmental pollution*, vol. 220, pp. 38–45, 2017.
- [36] J. P. McCracken *et al.*, "Longitudinal relationship between personal co and personal PM 2.5 among women cooking with woodfired cookstoves in Guatemala," *PloS one*, vol. 8, no. 2, p. e55670, 2013.
- [37] J. Li, X. Shao, and H. Zhao, "An online method based on random forest for air pollutant concentration forecasting," in *Chinese Control Conference*, 2018, pp. 9641–9648.
- [38] I. Turias, J. Jerez, L. Franco, H. MESA, J. Ruiz Aguilar, J. Moscoso, and M. Jimenez Come, "Prediction of carbon monoxide (CO) atmospheric pollution concentrations using meteorological variables," *WIT Transactions on Ecology and the Environment*, vol. 211, pp. 137–145, 04 2017.
- [39] E. Eslami, Y. Choi, Y. Lops, and A. Sayeed, "A real-time hourly ozone prediction system using deep convolutional neural network," *Neural Computing and Applications*, vol. 32, pp. 1–15, 07 2020.
- [40] Z. Qi *et al.*, "Deep air learning: Interpolation, prediction, and feature analysis of fine-grained air quality," *IEEE Transactions on Knowledge and Data Engineering*, vol. 30, no. 12, pp. 2285–2297, 2018.
- [41] S. Michaelides, D. Paronis, A. Retalis, and F. Tymvios, "Monitoring and forecasting air pollution levels by exploiting satellite, ground-based, and synoptic data, elaborated with regression models," *Advances in Meteorology*, vol. 2017, 2017.